TELKOMNIKA Indonesian Journal of Electrical Engineering
Vol. 12, No. 11, November 2014, pp. 7854 ~ 7862
DOI: 10.11591/telkomnika.v12i11.6024

Fault Diagnosis of Tuning Area Based on Wavelet Neural Network

Dong Yu*[1], Li Ya-Lan[1], Nan Jie-Nong[2]
[1]School of Automation and Electrical Engineering, Lanzhou Jiaotong University, Lanzhou 730070, China;
[2]Rail Department, Nanjing NRIET Industrial Co., Ltd. Nanjing 211100, China)
*Corresponding author, e-mail: 632745140@qq.com

Abstract
With the rapid development of china railway, ZPW-2000A track circuit has been widely used. Tuning area, which is an important part of the ZPW-2000A track circuit, is not only the relationship between the signal transmission qualities, and determines the effect of electrical insulation between adjacent sections. Therefore, the study of fault diagnosis aspects for tuning area is urgent and significant. In this paper, using the theory of transmission line a model of track circuit is built, the comparison of the actual data and experimental data of the track surface voltage envelope curve shows the correctness of this model. Owning to the good time-frequency characteristics of wavelet and the nonlinear mapping features of neural network, a fault diagnosis of ZPW-2000A tuning area based on the wavelet neural network (WNN) is proposed. Combined with the practical failure situation of railway site, the fault diagnosis method in this paper can accurately identify failure modes of tuning area.

Keywords: *ZPW-2000A track circuit, tuning area, fault diagnosis, wavelet neural network*

1. Introduction

With the rapid spread of ZPW-2000A track circuit, which has been used as the section block signaling equipment in the normal operation of the whole road was universal application. Therefore, the normal operation of the equipment is crucial for transportation and production. From the current point of the actual survey, the track circuit failures are mainly concentrated in the tuning unit disconnected, broken or capacitance value decreases of compensation capacitor and poor insulation of rail-to-ground ect. Among them, the fault of tuning unit will reduce the input signal voltage of track circuit receiver causing a feint of track occupied which is seriously affect driving efficiency. Moreover, If the train received a signal of adjacent track circuit which is beyond its transmission range since the tuning unit failure, and thus the signal decoded, this will cause a emergency braking because the speed of the train exceeds the speed limit value, as we all know, this is very dangerous. In summary, the impact caused by the failures of tuning unit is more serious on train operation, therefore, it is necessary to study the fault diagnosis method of tuning unit.

In china, the study in fault diagnosis of tuning area has not been expanded in-depth, so it is very valuable to conduct research in this area. This paper presents a method for fault diagnosis in tuning area based on wavelet neural network (WNN). Currently, there are two binding mode of wavelet analysis and neural networks: one way is a combination of wavelet transform with conventional neural network, typically using wavelet analysis of signal preprocessing, and then use conventional neural network learn and discriminate; another way is a synthesis of wavelet analysis and feedforward neural networks, namely, wavelet analysis is integrated into the neural network computing. In this paper both methods are used. Experimental results show: the two methods both can achieve fault detection and location with high accuracy.

2. Modeling of ZPW-2000A Track Circuit

ZPW-2000A track circuit is constituted by two parts: the main track circuit and tuning area which is regard as a extension for the section train running. There are four carrier frequency of ZPW-2000A track circuit: 1700, 2000, 2300, 2600, and that is arranged alternately

Received March 27, 2013; Revised May 30, 2014; Accepted June 15, 2014

in 1700 and 2300 for the downlink, while carrier frequency 2000 and 2600 is disposed alternately in the uplink. As the rail presents inductive properties, the compensation capacitor are arranged at equal distances in a parallel way to reduce the attenuation of the signal transmission process, what's more, the capacitor value of compensation capacitor is varies due to the different carrier frequency. The length of tuning region is 29m, and it is composed by the F1-type tuning unit (BA1), air coil, F2-type tuning unit (BA2) and the rails between them, as shown in Figure 1. For low carrier frequency section deploy F1-type, while high frequency section deploy F2 type [1]. Tuning unit shows the parallel resonance for this section signal to reduce the attenuation of the signal power, at the same time, a series resonance for adjacent segment signal to prevent cross-border transmission of signal.

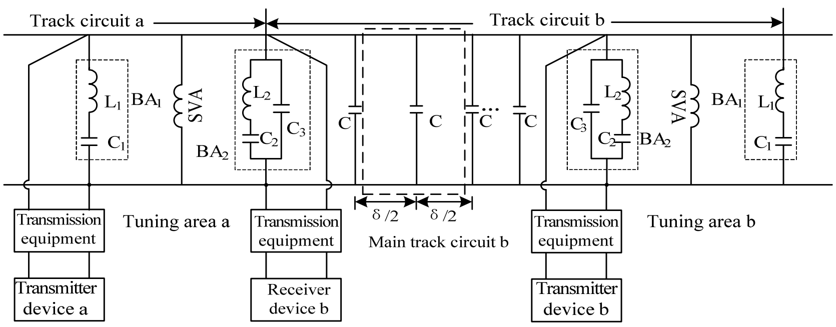

Figure 1. System Configuration of ZPW-2000A Track Circuit

As shown in Figure 1, compensation capacitor is set up for equidistant method, and the first compensation capacitor from the beginning of the track circuit as δ / 2m, as well as the last one from the track circuit terminal is δ / 2m , while the distance between the other compensation capacitor is δm. Assuming that the δ / 2m track circuit is equivalent to a four-terminal network, to compensation capacitance for the same equivalent. The dashed box in Figure 1 is a four terminal network unit(T_{ZF}^{b}) for the main track circuit, if the number of compensation capacitor is N, then the equivalent network of main track b is cascaded by the same number four-terminal network [2-3]. The equivalent parameters of the four terminal network unit is:

$$T_{ZF}{}^{b} = T_{gd}(\frac{\delta}{2}) \times T_{c} \times T_{gd}(\frac{\delta}{2}) \quad (1)$$

Where T_{gd} is the transmission parameters of track four-terminal network, T_C is the transmission parameters of compensation capacitor four-terminal network.

$$T_{gd} = \begin{bmatrix} \cosh(\gamma l) & Z_c \sinh(\gamma l) \\ \sinh(\gamma l)/Z_c & \cosh(\gamma l) \end{bmatrix} \quad T_c = \begin{bmatrix} 1 & 0 \\ j2\pi f_0 C & 1 \end{bmatrix} \quad (2)$$

In Equation (2), l represents the length of the track quadripole, γ represents the propagation constant of track circuit, Z_C is the characteristic impedance of the rail, C denotes the capacitor value of compensation capacitor, f_0 denotes the carrier frequency of transmission signal. So the equivalent network of the main rail b is:

$$T_Z^{b}=(T_{ZF}^{b})^N \quad (3)$$

For the equivalent network of tuning area b, each of the tuning unit and the air coil will be considered as a quadripole, which combin with the track four-terminal network between them make up the tuning area. The transmission parameters is:

$T_{TX}^{b}=T_{F1}\times T_{gd}\,(l_T/2)\times T_{SVA}\times T_{gd}(l_T/2)\times T_{F2}$ (4)

Where T_{F1} is the transmission parameters of F1-type tuning unit (BA1), T_{gd} denotes the transmission parameters of track four-terminal network between tuning area and air coil, l_T is the length of tuning area, T_{SVA} is the transmission parameters of air coil quadripole, T_{F2} represents the transmission parameters of F2-type tuning unit (BA2).

$$T_{F1}=\begin{bmatrix}1 & 0\\ \dfrac{1}{Z_{BA1}} & 1\end{bmatrix}\quad T_{SVA}=\begin{bmatrix}1 & 0\\ \dfrac{1}{Z_{SVA}} & 1\end{bmatrix}\quad T_{F2}=\begin{bmatrix}1 & 0\\ \dfrac{1}{Z_{BA2}} & 1\end{bmatrix} \tag{5}$$

Where Z_{BA1} is the pole impedance of F1-type tuning unit (BA1), Z_{SVA} is the impedance of air coil, Z_{BA2} is the zero impedance of F2-type tuning unit (BA2).

Take the section in 1700HZ carrier frequency for example, its rail impedance(Z) and ballast resistor(R_d) are as follows:

$Z=15.1\angle 82.3°\ \Omega/\text{km}\qquad R_d=1\Omega\cdot\text{km}$ (6)

The propagation constant and characteristic impedance of the rail are shown below [4-5]:

$$\gamma=\sqrt{\left|Z/R_d\right|}\angle\frac{\phi_Z}{2}=2.926+\text{j}2.557\qquad Z_c=\sqrt{\left|Z\cdot R_d\right|}\angle\frac{\phi_Z}{2}=2.926+\text{j}2.557 \tag{7}$$

Since the length of tuning area is 29m, in equation (4), l_T is 29m, substituting into Equation (2), the coefficient of T_{gd} ($l_T/2$) is follows:

$$0.0145\gamma=(2.926+\text{j}2.557)\times 0.0145=0.0424+\ \text{j}0.0371$$
$$\cosh(0.0145\gamma)=1.0002+\text{j}0.0016$$
$$\sinh(0.0145\gamma)=0.0424+\text{j}0.0371$$
$$T_{gd}=\begin{bmatrix}1.0002+j0.0016 & 0.0292+j0.2170\\ 0.0145 & 1.0002+j0.0016\end{bmatrix}$$

As the train entering the section, the track circuit displays shunt status. When the train enters the i-th four-terminal network, namely the location of the i-th compensation capacitor (T_{ZFi}^{b}), then the main track is equivalent to a four-terminal network cascaded by the i-th four-terminal network and the rest of four-terminal network number for N-i. Presuming that the location of branching point from the beginning of the i-th four-terminal network is x, then the i-th four-terminal network is divided into the following three conditions as shown in Figure 2: shunting point on the left of compensation capacitor, the shunting point at compensation capacitor, the shunting point on the right of compensation capacitor.

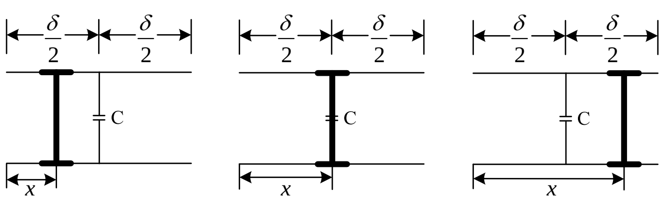

Figure 2. Distribution of Shunting Point in the i-th Quadripole

From the Figure 2, the transmission parameters of i-th four-terminal network is:

$$T_{ZFi}{}^{b} = \begin{cases} T_{gd}(\frac{\delta}{2} - x) \times T_c \times T_{gd}(\frac{\delta}{2}) & x < \frac{\delta}{2} \\ T_c \times T_{gd}(\frac{\delta}{2}) & x = \frac{\delta}{2} \\ T_{gd}(\delta - x) & x > \frac{\delta}{2} \end{cases} \quad (8)$$

At this point, the entire main rail equivalent to a four-terminal network cascaded by the i-th four-terminal network ($T_{ZFi}{}^{b}$) with the rest four-terminal networks in N-i numbers. The transmission parameters is:

$$T_Z{}^{b} = T_{ZFi}{}^{b} \times \left(T_{ZF}{}^{b}\right)^{N-i} \quad (9)$$

The length of 10km transmission cable can be seen as a uniform transmission line [6], its transmission matrix is the same as formula (2).

In a four-terminal network, the relationship between the two port voltage and current can be expressed by the following equation:

$$\begin{cases} \dot{U}_1 = A\dot{U}_2 + B\left(\dot{I}_2\right) \\ \dot{I}_1 = C\dot{U}_2 + D\left(\dot{I}_2\right) \end{cases} \Leftrightarrow \begin{bmatrix} \dot{U}_1 \\ \dot{I}_1 \end{bmatrix} = \begin{bmatrix} A & B \\ C & D \end{bmatrix} \begin{bmatrix} \dot{U}_2 \\ \dot{I}_2 \end{bmatrix} \quad (10)$$

When calculating the voltage at any point in the track surface, the entire section is divided into two parts, left and right, such as Figure 3.

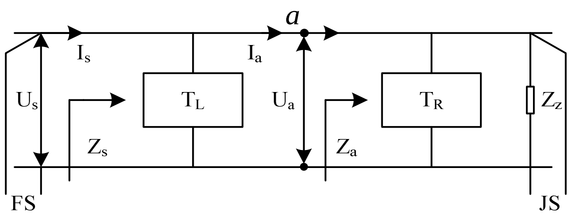

Figure 3. Equivalent Network at any Point (a point)

The input impedance to the right of the four-terminal network T_R is:

$$Z_a = \frac{T_{R11} \times Z_z + T_{R12}}{T_{R21} \times Z_z + T_{R22}} \quad (11)$$

Where Z_z is the input impedance of the receiver. For the left four-terminal network T_L, there are voltage-current relationship:

$$\begin{cases} U_S = T_{L11} \times U_a + T_{L12} \times I_a \\ I_S = T_{L11} \times U_a + T_{L21} \times I_a \end{cases} \quad (12)$$

According to voltage-current relationship of a point: Ua=Ia×Za, a point current is calculating as:

$$I_a = \frac{U_S}{T_{L11} \times Z_a + T_{L12}} \quad (13)$$

Thus, voltage of rail surface in any point is:

$$U_a = I_a \times Z_a \quad (14)$$

This paper calculate the voltage of rail surface based on the above formula, the simulation results of rail surface voltage and residual voltage of shunting are shown in Figure 4 and Figure 5.

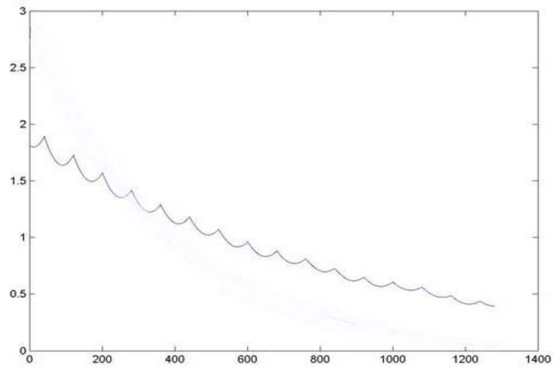

Figure 4. Voltage of Rail Surface

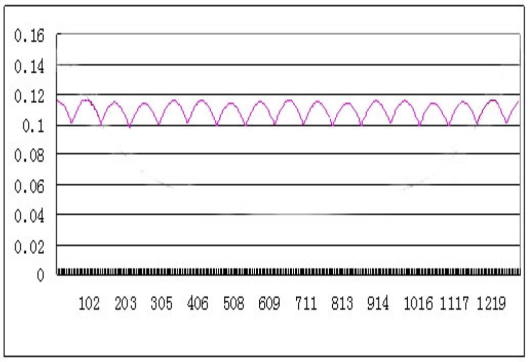

Figure 5. Residual Voltage of Train Shunting

In Figure 1, when the tuning unit BA1 breakdown, for track circuit a, the corresponding parallel resonance relationship is destroyed, and the series resonance effect of segment a formed by the BA2 still exists, so the signal in track circuit a is not transmitted across its range. When the failure occurred in tuner unit BA2, for track circuit b, the corresponding parallel resonance relationship is destroyed, but the series resonant relationship constituted by BA1 is being, as a result, the phenomenon in section b of beyond the transmission doesn't occur; while section a, its corresponding series and parallel resonance relations have been destroyed, which lead to the signal of section a transmitted into section b until it reaches the tuning area BA2 of section b presenting its series resonance characteristics for the signal. When these conditions occured, the transmission parameters for the entire network have been changed.

3. Fault Diagnosis Based on WNN

3.1. Basic Principles of WNN

In recent years, signal processing and fault diagnosis technologies based on wavelet analysis have achieved good results with the constant improvement and rapid development of wavelet theory. The wavelet transform is a new conversion method developed on the basis of the short-time fourier transform which have the characteristic of multi-resolution analysis and strong ability of characterizing the local features of signal both in time domain and frequency domain.

Wave wavelet is present in a smaller area. The mathematical definition of wavelet function is: let $\psi(t)$ is a square-integrable functions, that is $\psi(t) \in L^2(R)$, if its fourier transform meet the following conditions:

$$C_\psi = \int_R \frac{\left|\overline{\psi}\left(\overline{\omega}\right)\right|^2}{|\omega|} d\omega < \infty \quad (15)$$

In this case, $\psi(t)$ is a basic wavelet or mother wavelet, saying the formula (15) is permissible condition of wavelet function. Taking stretching and translation of the mother wavelet function $\psi(t)$, then generates a wavelet sequence. Namely:

$$\psi_{a,b}(t) = |a|^{-\frac{1}{2}} \psi\left(\frac{t-b}{a}\right) \qquad a, b \in R \, ; a \neq 0 \tag{16}$$

Where a is a stretching factor (also known as scale factor), b is the translation factor, $\psi_{a,b}(t)$ is a wavelet function.

In the case of the discrete, wavelet sequence is:

$$\psi_{j,k}(t) = 2^{-j/2}\psi(2^{-j}t - k) \qquad j, k \in Z \tag{17}$$

The continuous wavelet transform for any function $f(t) \in L^2(R)$ is:

$$W_f(a,b) = < f, \psi_{a,b} > = |a|^{-1/2} \int_R f(t) \cdot \overline{\psi\left(\frac{t-b}{a}\right)} dt \tag{18}$$

Figure 6 is the most significant and versatile representative for 3-layer feedforward BP neural network model, which is composed by input layer, output layer and several hidden layers. It should be noted that neurons in the same layer don't connect each other and the adjacent layers connected by weights. In Figure 6, x_j represents a input of the j-th input layer node, ω_{ij} represents the hidden layer weights between j-th input layer node and i-th hidden layer node, θ_i represents the threshold of i-th hidden layer node, $\phi(x)$ represents activation function in the hidden layer, ω_{ki} represents the weights between k-th output layer node and i-th hidden layer node, a_k means the threshold of k-th output layer node, $\psi(x)$ denotes activation function in the output layer, O_k denotes the output of the k-th output layer node.

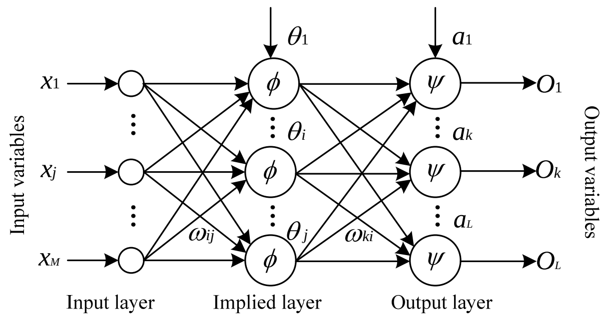

Figure 6. The Model of 3-layer BP Neural Network

The training process of BP network is: firstly, calculating the output of each node positively, then calculating the error based on actual output, finally, adjusting weights between the hidden layer and output layer as well as the weights between the input layer and the hidden layer in turn according to BP error rule, in order to reduce the error, making the network outputs meet expectations.

When BP network training, the number of hidden layer and nodes on each, the activation function and samples for input/output must have been specified. This is because these parameters will affect the convergence rate and effectiveness of the BP network. The number of hidden nodes is given by the empirical formula:

$$H \geq \sqrt{M + L} + a \tag{19}$$

Where M is the number of input neurons, L is the number of output neurons, a is a constant between 1 and 10.

Wavelet transform has advantage of time-frequency characteristics of local and zoom features, while neural networks can achieve satisfactory performances, such as strong character of robustness, fault tolerance and studies ability independently, and how to combine the advantages of both has been an issue that people care about. In fact, They combine with each other in two ways: one kind is auxiliary combination way, which use wavelet analysis preprocess signal preprocess, then the task of learning and discrimination transmit to the neural network; another approach is compact structure (or nested combination), that is blending the wavelet algorithm in neural network to form a wavelet neural network. In this paper, two methods were used respectively for fault diagnosis of tuning area.

3.2. Diagnostic Methods and Results

For the first binding mode, the characteristic vector of rail surface voltage is extracted by wavelet transform with time-frequency localization features, then making use of nonlinear mapping of BP network to classify feature vector in various state to implement fault diagnosis of tuning area. Its structural principle is shown in Figure 7.

Figure 7. The Diagnostic Process of First Structure

The second combination way is to replace the nonlinear activation function of neurons of nonlinear wavelet basis function, in this article, this article Morlet mother wavelet function was selected as the activation function of hidden layer. The structural process of the second way is shown in Figure 8.

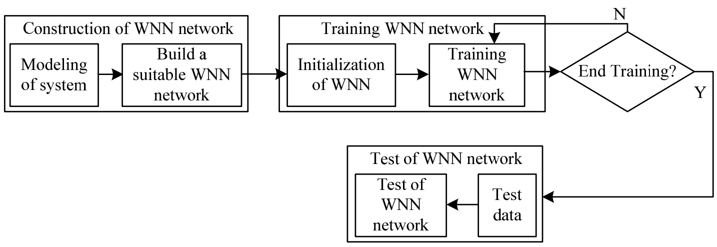

Figure 8. The Diagnostic Process of Second Structure

BP algorithm has the essence of solving the minimum error function, but there is a problem of low learning efficiency, slow convergence and easy to fall into local minimal state because it uses steepest descent method in nonlinear programming which modify the weights according to the negative gradient direction of the error function. For above shortcomings, the following improvements have two methods: additional momentum and adaptive learning rate.

Regulating formula for weights and thresholds with additional momentum factor is:

$$\begin{aligned} \Delta\omega_{ij}(k+1) &= (1-mc)\eta\delta_i p_j + mc\Delta\omega_{ij}(k) \\ \Delta b_i(k+1) &= (1-mc)\eta\delta_i + mc\Delta b_i(k) \end{aligned} \quad (20)$$

Regulating formula for adaptive learning rate is:

$$\eta(k+1)=\begin{cases}1.05\eta(k) & E(k+1)<E(k)\\ 0.7\eta(k) & E(k+1)>1.04E(k)\\ \eta(k) & \text{others}\end{cases} \quad (21)$$

Where $E(k)$ is the sum of the squares of the errors in k-th step, η is the learning rate.

When using the additional momentum factor method, BP algorithm can find the global optimal solution, while reduce training time in adopting adaptive learning rate. When these two methods combined, momentum-adaptive learning rate adjustment algorithm is produced.

In this paper, BP neural network, improved BP neural network combined with wavelet separately by the two structure used for troubleshooting. Comparison of diagnostic result is shown in Figure 9 and Figure 10.

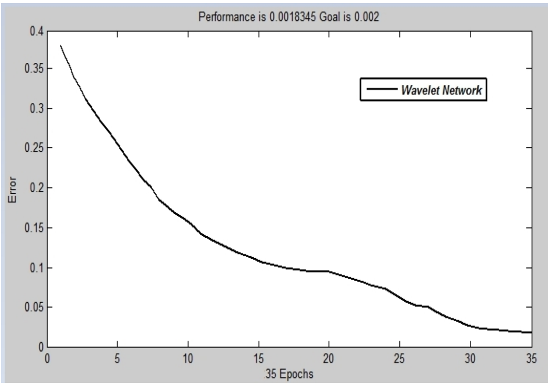

Figure 9. The Improved BP Network Combined with Wavelet in First Way

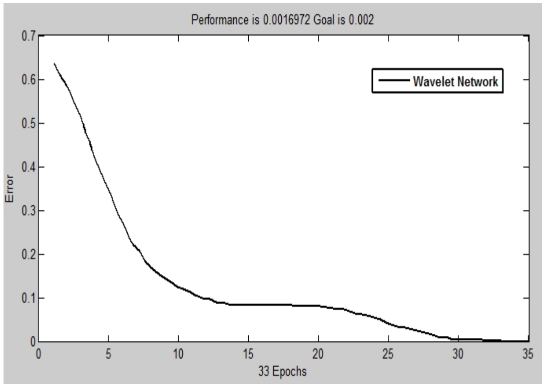

Figure 10. The Improved BP Network Combined with Wavelet in Second Way

As can be seen from the figures, with the first step structure of WNN only 35 steps need to meet the requirements of the predetermined error 0.002; while it only takes 33 steps to reach the pre-meet requirements error of 0.002 when adopting the second structure of WNN. By comparison, regardless of the first structure or the second structure, both of them can achieves the error requirement with fast convergence speed. Simultaneously, compared the speed of improved combination algorithm with the original one, as shown in Figure 11 and Figure 12.

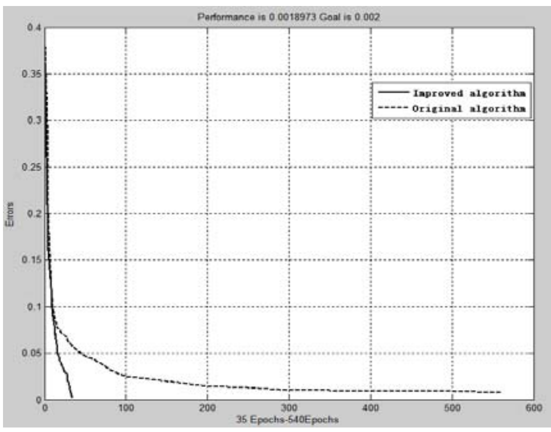

Figure 11. Comparison of First WNN for the Original Algorithm and Improved Algorithm

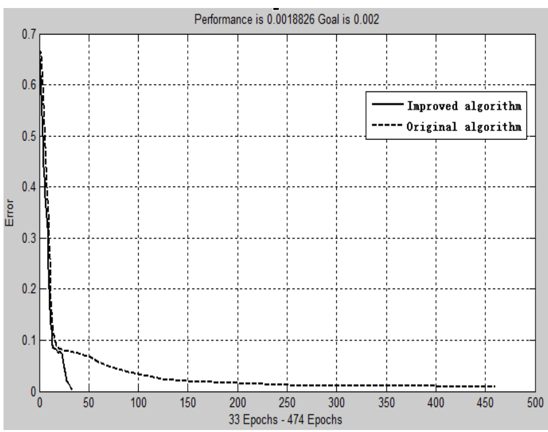

Figure 12. Comparison of Second WNN for the Original Algorithm and Improved Algorithm

As can be seen from the figures, the reduction of initial error in both two structures is quickly, but about 150 to 200 steps, downward trend in the training error becomes very slow, however, the improved algorithm to reduce the error rate has been very fast. Meanwhile, the introduction of momentum item avoid the occurrence of shock effectively and has a significant smoothing effect.

4. Conclusion

This paper combines wavelet transform and neural network, producing the wavelet neural network (WNN), and making full use of the advantages of them to diagnose ZPW-2000A track circuit tuning area. First of all, this thesis build the model of ZPW-2000A track circuit using transmission line theory and the voltage of rail surface along with residual voltage of train shunting are simulated. Then the BP neural network in conjunction with improved BP neural network are combined with wavelet analysis in two ways, forming different methods of fault diagnosis. Finally, use each method to diagnose tuning area. What's more, experimental results show that the WNN which formed by improved BP network and wavelet analysis is a more effective diagnostic methods. In addition, combined with on-site accident cases, the accuracy of this diagnostic method up to 98%.

References

[1] Fei Xikang. Principle and Analysis of Jointless Track Circuit. Beijing: China Railway Press. 1993: 17-91.
[2] Zhao L, Liu B, Xu X. *Using the wavelet analysis based noise canceling technique to detect the integrity of the compensating capacitors of UM71 track circuit*. IEEE 2005 International Symposium, on Microwave, Antenna, Propagation and EMC Technologies for Wireless Communications. 2005; 2: 1268-1274.
[3] Kim MS, Lee JW, Ko JS. *A study on the compensation capacitor in ballast track circuit*. International Conference on Electrical Machines and Systems, IEEE. 2008: 4182-4187.
[4] Jin Y, Zheng X, Ding T. *A high-accuracy parameter estimation algorithm for jointless frequency-shift track circuit*. International Colloquium on Computing, Communication, Control, and Management, IEEE. 2008; 1: 750-753.
[5] Minin VA, Johnston DA, Lepsky NA. *A general model for optimization of track circuit parameters*. Proceedings of the 1995 IEEE/ASME Joint Railroad Conference. 1995: 113-117.
[6] Nikolov N, Nedelchev N. Study on centre-fed boundless track circuits. *IEE Proceedings-Electric Power Applications*. 2005; 152(5): 1049-1054.